Dyes and Pigments 195 (2021) 109708

Contents lists available at ScienceDirect

Dyes and Pigments

journal homepage: www.elsevier.com/locate/dyepig

Mechanochromism, thermochromism, protonation effect and discrimination of $CHCl_3$ from organic solvents in a Et_2N-substituted Salicylaldehyde Schiff base

Jun Shu [a], Tong Ni [a], Xiaoqiang Liu [a], Bin Xu [a], Lang Liu [b], Wendao Chu [c], Kaiming Zhang [a,*], Weidong Jiang [a,**]

[a] Key Laboratory of Green Chemistry of Sichuan Institutes of Higher Education, School of Chemistry and Environmental Engineering, Sichuan University of Science & Engineering, Sichuan Zigong, 643000, PR China

[b] College of Chemistry, Xinjiang University, Urumqi, 830046, PR China

[c] Chemical Synthesis and Pollution Control Key Laboratory of Sichuan Province, College of Chemistry and Chemical Engineering, China West Normal University, Nanchong, 637002, PR China

ARTICLE INFO

Keywords:
Multi-stimuli response
Salicylaldehyde schiff base
Mechanochromism
Thermochromism
Protonation effect
Discrimination of $CHCl_3$

ABSTRACT

Multi-stimuli-responsive materials, which can show color/fluorescence change in response to external chemical or physical stimuli, have received increasing attention due to the capacities for facile realization of multifunctional sensing. Herein, we presented a Et_2N-substituted salicylaldehyde Schiff base compound (DDHAC) with multi-stimuli-responsive behaviors. An investigation of the photophysical properties in solution demonstrated DDHAC was an excited-state intramolecular proton transfer (ESIPT) and aggregation-induced emission (AIE) active molecule. Owing to structural flexibility from salicylaldehyde Schiff base, the compound displayed reversible mechanochromic and thermochromic behavior, which were associated with the crystalline-to-amorphous and crystalline-to-crystalline, respectively. Moreover, the Et_2N group endowed DDHAC with the capability that response of protonation. Due to its protonation effect, DDHAC could serve as a unique optical probe for discriminating $CHCl_3$ from organic solvents assisted by UV irradiation. The selectivity was attributed to the interaction of DPPTP with HCl gas from photodecomposition product of chloroform.

1. Introduction

Organic stimuli-responsive molecules can change their chemical or physical structures upon external stimuli and exhibit tunable emission and/or absorption properties. The smart materials have aroused enormous interest owing to their promising practical applications in detection of mechanical force [1–14], heat [15–22], acid/base [23–30], organic solvent [31–35] and so on. To date, a series of stimuli-responsive materials have been developed, and whereas most of which typically exhibit only single environmental stimuli response. Samples possessing multi-stimuli-responsive (MSR) capabilities are much less frequently reported. Normally, the integration strategy that installing distinct stimuli-responsive moieties and fluorophore into one system is employed to construct MSR polymers [36–43]. For example, Song and co-workers developed a novel MSR macromolecule through incorporation of diethylamino (pH/CO_2-responsive group) and acrylamide (thermoresponsive moiety) into homopolymer [41]. By tagging multi-function unit of cyanoethylene to a polymer, a smart mechano- and thermoresponsive material was achieved by Lavrenova and co-workers [42]. In most instances, however, the MSR polymeric materials always raise additional synthetic challenges [39]. By contrast, small organic molecules with simple structure could be preferred [44–48].

Salicylaldehyde-based Schiff base compound is a type of potential stimuli-responsive material because (1) it is easily synthesized and purified; (2) it often shows AIE attribute [49–54], which is suitable for monitoring stimuli-induced chromism in solid state; (3) more importantly, its structural flexibility [55,56] is beneficial to phase transition from one to another states and resultant tunable emission upon external stimuli. Indeed, its derivatives have been extensively used for detection

* Corresponding author.
** Corresponding author.
E-mail addresses: susezkm@163.com (K. Zhang), jwdxb@suse.edu.cn (W. Jiang).

https://doi.org/10.1016/j.dyepig.2021.109708
Received 4 May 2021; Received in revised form 5 August 2021; Accepted 6 August 2021
Available online 8 August 2021

of mechanical force, heating, cations, anions and enzymes [12–16, 57–62]. However, little effort has been made to exploit their capacity in multi-parameter sensing.

In this study, we reported a multi-stimuli-responsive compound DDHAC with Et_2N-substituted salicylaldehyde Schiff base skeleton (Scheme 1). Due to the structural flexibility from salicylaldehyde Schiff base, this molecule showed mechanochromism and thermochromism behavior. Moreover, the introduction of the Et_2N group endowed DDHAC with the capability that response of protonation, further allowed it to discriminate $CHCl_3$ from organic solvents assisted by UV irradiation.

2. Experimental

2.1. Measurements and material

All reagents and solvents were purchased from commercial sources and used as received without further purification. ^{1}H and ^{13}C NMR spectra were recorded on a Bruker AV III HD 600 spectrometer. LRMS and HRMS were obtained on Bruker micrOTOF-Q-II and Bruker SolariX-70FT mass spectrometer, respectively. UV–Vis spectra were recorded on a Purkinje TU-1950 spectrophotometer. Photoluminescence (PL) spectra were recorded on an Agilent Cary Eclipse fluorescence spectrophotometer. The fluorescence quantum yields in solutions were measured by comparing a standard (fluorescein in 0.1 N NaOH aqueous solution, Q_F = 0.79). The absolute fluorescence quantum yields of solids were measured on a Hamamatsu C9920-02G spectrometer. The X-ray diffraction (XRD) measurements were carried out on a Skyray DX-2600 X-ray diffractometer. The emission spectra were measured under excitation at 415 nm. The photographic images were taken under a 365 nm UV lamp.

Preparation of the samples for photophysical properties study. The UV–Vis absorption and PL spectra of DDHAC in various organic solvents were measured using freshly prepared 1.0×10^{-5} M solutions. The CH_3CN/water (or THF/CH_3OH) mixtures (concentration of 1.0×10^{-5} M) with different water (or CH_3OH) fractions were prepared by slowly adding distilled water into the CH_3CN (or THF) solution of sample under ultrasound at room temperature.

2.2. Synthesis

Synthesis of 7-diethylamino-3-nitrocoumarin. 4-diethylamino-2-hydroxybenzaldehyde (2.50 g, 13 mmol) was dissolved in n-BuOH (40 mL), ethyl nitroacetate (2.39 g, 18 mmol) and piperidine (0.4 mL) was added, and the mixture was refluxed for 12 h. After cooling to room temperature, orange crystals precipitated out from the mixture and they were filtered off and washed with cold n-BuOH and diethyl ether to yield 7-diethylamino-3-nitrocoumarin as orange solid (1.89 g, 56 %), m. p. 205.4–206.1 °C. ^{1}H NMR (600 MHz, $CDCl_3$) δ 8.67 (s, 1H), 7.43–7.40 (m, 1H), 6.69 (dd, J = 9.1, 2.4 Hz, 1H), 6.44 (d, J = 2.3 Hz, 1H), 3.48 (q, J = 7.2 Hz, 4H), 1.25 (t, J = 7.2 Hz, 6H). ^{13}C NMR (151 MHz, $CDCl_3$) δ 158.82, 154.71, 153.57, 143.43, 132.71, 126.69, 111.35, 106.29, 96.81, 77.37, 77.16, 76.95, 45.65, 12.49. IR (KBr pellet): 2979(w), 1745(s), 1629(s), 1507(m), 1326(m), 1255(m), 823(w) cm^{-1}. HRMS (ESI): m/z $[M+H]^+$ calcd. for $[C_{13}H_{15}N_2O_4]^+$ 263.1032, found 263.1019.

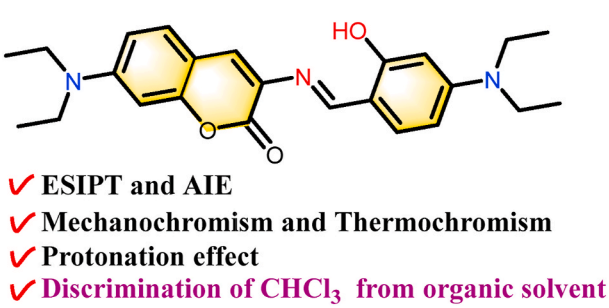

Scheme 1. The molecular structure and multi-stimuli responses of DDHAC.

Synthesis of 3-amino-7-diethylaminocoumarin. Stannous chloride dihydrate (11.36 g, 50.33 mmol) was added in conc. HCl (35 mL). To this suspension 7-diethylamino-3-nitrocoumarin (1.76 g, 6.7 mmol) was added at 0 °C in small portions, over a period of 1 h. The mixture was stirred for 4 h at room temperature and then diluted in iced water (300 mL). The pH was adjusted to 8 with NaOH and the mixture was extracted three times with ethyl acetate (100 mL) at a time. The combined organic layers were dried over Na_2SO_4 and the solvent was evaporated in vacuum to obtain 3-amino-7-diethylaminocoumarin as pale yellow solid (1.29 g, 83 %), m. p. 90.4–91.2 °C. ^{1}H NMR (600 MHz, $CDCl_3$) δ 7.09 (d, J = 8.7 Hz, 1H), 6.69 (s, 1H), 6.56 (d, J = 8.5 Hz, 1H), 6.51 (s, 1H), 3.90 (s, 2H), 3.35 (q, J = 7.1 Hz, 4H), 1.16 (t, J = 7.1 Hz, 6H). ^{13}C NMR (151 MHz, $CDCl_3$) δ 160.42, 151.66, 147.48, 127.65, 126.05, 114.52, 109.83, 109.47, 98.10, 44.75, 12.55. IR (KBr pellet): 3372 (double, w), 2970(w), 1697(s), 1623(s), 1589(m), 1326(m), 1129(m), 816(w) cm^{-1}. HRMS (ESI): m/z $[M+H]^+$ calcd. for $[C_{13}H_{17}N_2O_2]^+$ 233.1290, found 233.1277.

Synthesis of DDHAC. To a stirred solution of 3-amino-7-diethylaminocoumarin (464 mg, 2 mmol), 4-(diethylamino)-2-hydroxybenzaldehyde (425 mg, 2.2 mmol) in EtOH (16 mL) were added CH_3COOH (0.5 mL). The mixture was stirred for 2 h at room temperature and then filtered off to obtain red solid. Further purification was performed by recrystallization from THF to yield DDHAC as yellow solid (627 mg, 77 %), m. p. 238.2–238.8 °C. ^{1}H NMR (600 MHz, DMSO-d_6) δ 13.63 (s, 1H), 8.94 (s, 1H), 7.81 (s, 1H), 7.44 (d, J = 8.9 Hz, 1H), 7.26 (d, J = 8.9 Hz, 1H), 6.73 (dd, J = 8.9, 2.3 Hz, 1H), 6.57 (d, J = 2.2 Hz, 1H), 6.31 (dd, J = 8.9, 2.3 Hz, 1H), 6.06 (d, J = 2.2 Hz, 1H), 3.47–3.35 (m, 8H), 1.12 (td, J = 7.0, 4.6 Hz, 12H). ^{13}C NMR (151 MHz, DMSO) δ 163.41, 160.61, 158.79, 154.14, 151.49, 149.67, 133.92, 129.22, 129.05, 126.94, 109.41, 108.82, 108.22, 103.95, 96.93, 96.47, 44.06, 43.92, 12.57, 12.37. IR (KBr pellet):3441 (br, m), 2971(w), 1700(s), 1615(s), 1511(m), 1343(m), 1238(m), 1129, 819(w) cm^{-1}. HRMS (ESI): m/z $[M+H]^+$ calcd. for $[C_{24}H_{30}N_3O_3]^+$ 408.2287, found 408.2259.

3. Results and discussion

3.1. Synthesis and characterization

The synthetic routes were illustrated in Scheme S1. The reaction of starting compound 4-diethylamino salicylaldehyde with ethyl nitroacetate in the presence of piperidine as catalyst gave 7-diethylamino-3-nitro coumarin, which was further reduced by stannous chloride to 3-amino-7-diethylamino coumarin [63]. Compound 3-amino-7-diethylamino coumarin could be easily converted to target compound DDHAC by condensation reaction with 4-diethylamino salicylaldehyde. ^{1}H NMR, ^{13}C NMR and MS-ESI were carried out to confirm the molecular structures.

3.2. ESIPT properties

Owing to the rotation of central C–C single bond connecting the phenyl and imino group, there were two species for compound DDHAC in solution including open-enol and hydrogen-bonded enol forms [64] (Scheme 2). The former displayed normal emission; the latter could undergo the excited-state intramolecular proton transfer (ESIPT) process after photoexcitation, and exhibited keto-form emission based on a keto-enol tautomerization. Therefore, the dual emission bands were observed for DDHAC in solution (Table 1). For example, clearly double-peaked bands were found in PL spectra in n-hexane, toluene, tetrahydrofuran, ethyl acetate and chloroform (Fig. 1b). One was the normal emission in short-wavelength region, and the other was the keto-form emission after the ESIPT process in long-wavelength region. However, only single-peaked broad emission bands were observed in

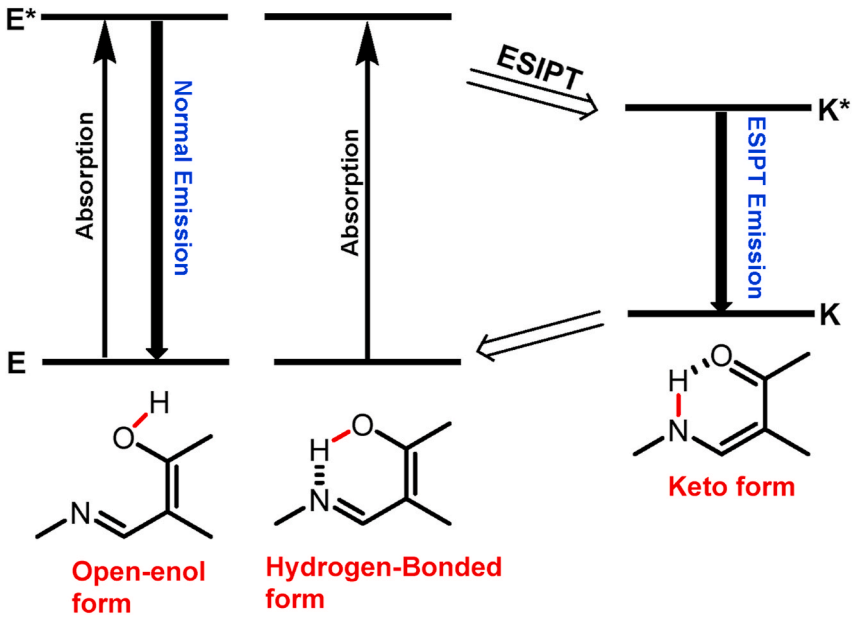

Scheme 2. General representation of the ESIPT Process.

Table 1
Photophysical data of DDHAC in various solvents.

Solvent	λ_{Abs} (nm)	λ_{PL} (nm)	Φ_F (%)
n-hexane	425, 451	468, 500	3.87
toluene	437, 460	490, 508	8.28
ethyl acetate	436, 455	493, 509	7.88
tetrahydrofuran	439, 459	495, 516	9.65
chloroform	442, 464	513, 550	21.24
acetone	458	513	8.11
acetonitrile	458	536	7.51
methanol	469	561	36.28

[a] Only the absorption/emission peaks wavelengths were shown.
[b] Emission spectra were performed upon excitation at 415 nm.

acetone and acetonitrile. It was because the intramolecular hydrogen bonding (-OH···N-) could be interrupted by polar solvents [64], and the open-enol form of DDHAC was the dominant species. It was noted that DDHAC emitted weak fluorescence in the majority of organic solvents, and non-radiative relaxation of excited states from the intramolecular rotation [51] or solvent relaxation [65] could account for the phenomenon. Furthermore, DDHAC displayed dual absorption peaks in n-hexane, toluene, tetrahydrofuran, ethyl acetate and chloroform (Fig. 1a), where the shorter absorption band was ascribed to coumarin structure and the longer absorption band was assigned to the coupling between coumarin and the hydroxyphenyl ring.

3.3. AIE properties

To investigate the fluorescent behavior of DDHAC in aggregation state, the emission spectra in CH_3CN/water mixtures with different fractions of water (f_w) were performed (Fig. 2a). DDHAC emitted a weak emission in strong polar solvent CH_3CN. However, the fluorescence was enhanced gradually by increasing the f_w, and reached the intensity maximum at 0.4 of water content, revealing the AIE characteristic of DDHAC. From 0.4 to 0.9 of f_w, DDHAC displayed reduction of emission intensity, which could be attributed to the formation of nanoparticles in a higher water faction. The aggregation of DDHAC in CH_3CN/water system was supported by absorption spectra and dynamic light scattering (DLS) measurements. As shown in Fig. 2c, in the absorption spectra, a level-off tail in the long-wavelength region could be obviously observed in 40 % water/THF (v/v) solution, which was caused by light scattering effect of aggregate suspensions. DLS measurements revealed that the particle size was around 100 nm (Fig. 2c inset). Additionally,

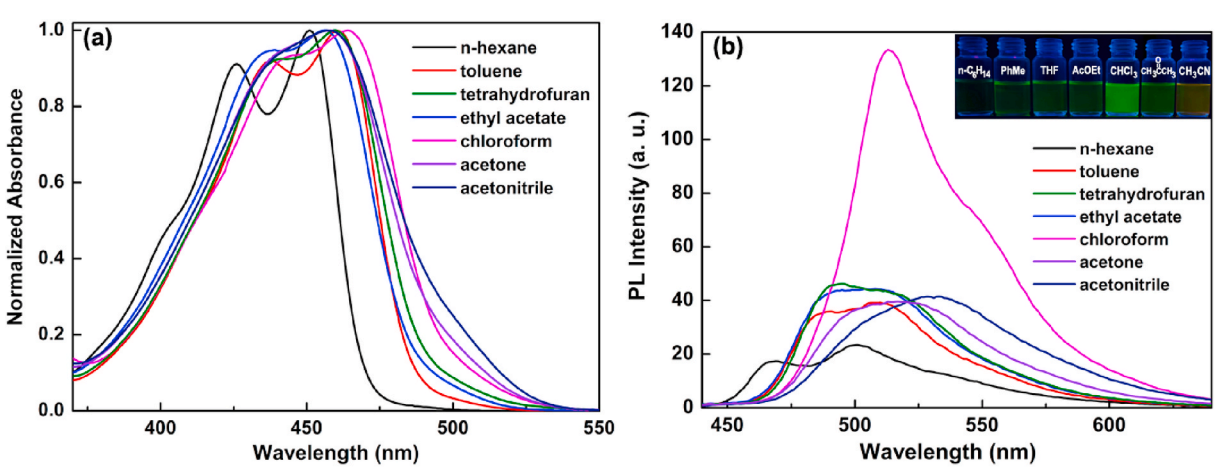

Fig. 1. (a) Normalized absorption spectra and (b) PL spectra and photographic images (inset) of DDHAC in various solvents.

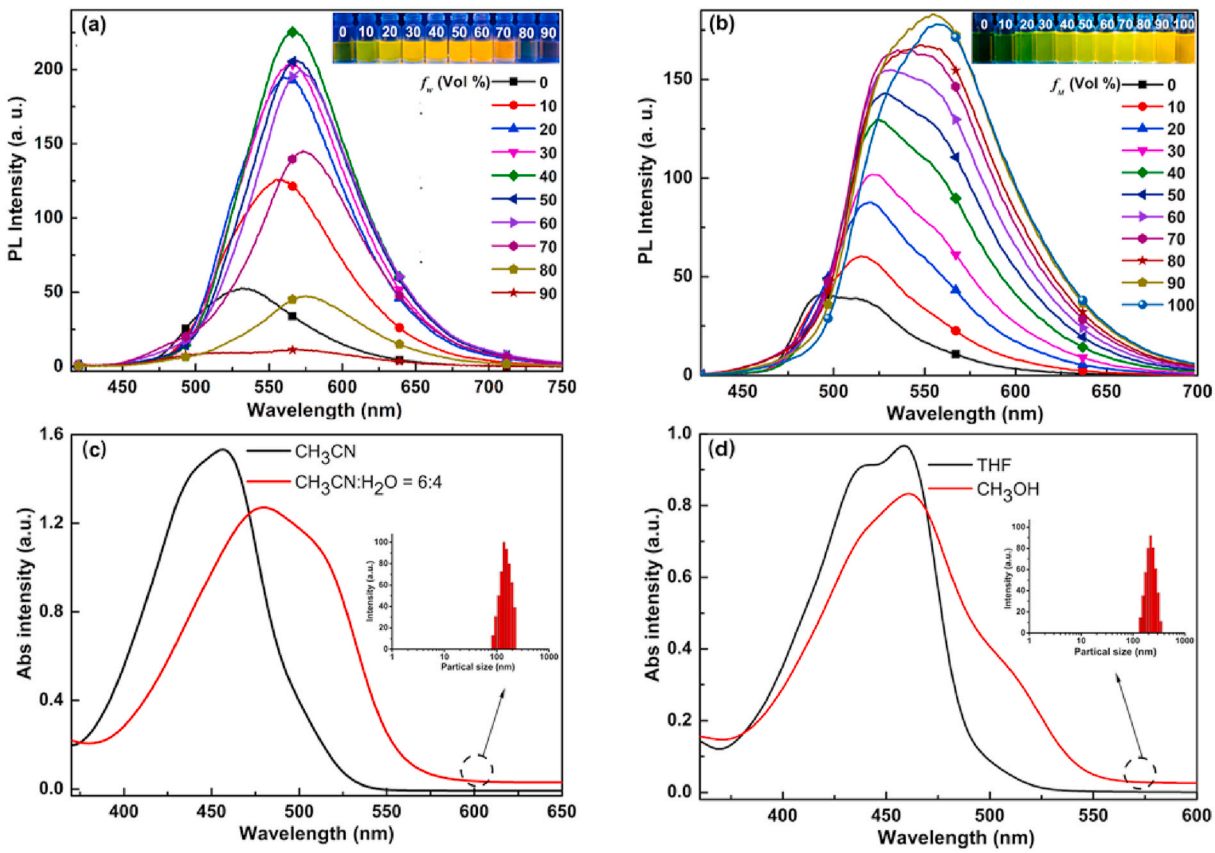

Fig. 2. Fluorescence spectra and emission images (insets) of DDHAC in (a) CH_3CN/water and (b) THF/CH_3OH mixtures; absorption spectra and DLS results (insets) of DDHAC in (c) 40 % CH_3CN/water (v/v) mixture and (d) CH_3OH.

AIE properties of DDHAC were examined in THF-CH_3OH systems with different methanol fractions (f_M) (Fig. 2b and d). In a good solvent of THF, DDHAC exhibited very weak fluorescence. After the addition of MeOH, a poor solvent for Schiff base dye, into the THF solution, the emission intensity enhanced gradually, and reached the maximum at 0.90 of f_M. Similarly, absorption spectra and DLS of CH_3OH solution also indicated that the aggregates were generated. The AIE properties could be attributed to restriction of the intramolecular rotation (RIR) and torsion effect [53,66].

3.4. Mechanochromism and thermochromism behavior

Considering that structural flexibility of salicylaldehyde imine, the mechanochromism and thermochromism behavior of DDHAC were performed. As shown in Fig. 3a, the pristine powders obtained by crystallization in THF solution emitted bright yellow emission (Φ_F = 11.7 %) with double peaks at 566 nm and 587 nm (black line). Once original powders were ground using a pestle and mortar, the resultant samples showed weak fluorescence (Φ_F = 2.8 %) with single peak located at 597 nm (red line). The fluorescence could be recovered to its original state by fuming with THF (pink line), suggesting the reversible mechanical stimuli-response behavior. Furthermore, by heating pristine

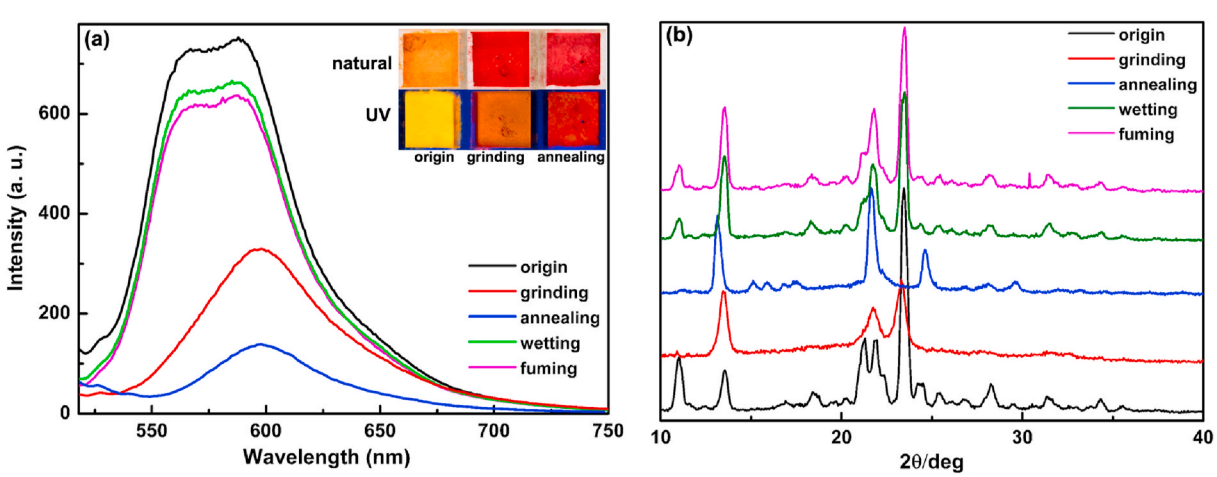

Fig. 3. (a) Emission spectra and (b) XRD patterns of the corresponding samples for DDHAC. Inset: natural and fluorescent images of DDHAC in different states.

samples at 180 °C for 30 s and cooling to room temperature, the resultant annealed samples presented single emission peak at 599 nm with weaker intensity ($\Phi_F = 1.5$ %) compared to that of ground powders (blue line); the emission of annealed powders also returned to original state by wetting with THF (green line), indicative of reversible thermal stimuli-response behavior.

Powder X-ray diffraction (PXRD) measurements were carried out to understand the mechanical and thermal effects on the material (Fig. 3b). The diffraction curves of original powder displayed sharp and intense reflections, indicating well crystalline order. The diffraction peaks of ground samples were obviously diminished or disappeared relative to those of original powder, implying disordered molecular packing [7,9, 14]. In the case of annealed powders, the PXRD pattern still revealed obvious crystalline structure features, but it was quite different from origin. These results demonstrated that annealing treatment should result in another crystalline formation of DDHAC [67]. Differential scanning calorimetry (DSC) measurements further proved this inference (Fig. S1). DSC curves of origin powder showed an endothermic transition peak at 176 °C before the melting point at 238 °C, By contrast, melting peak shifted to 236 °C and first endothermic peak vanished for annealing powder, suggesting the formation of new crystalline phase unlike that of origin [16]. When the ground and annealed powders were treated with THF, both of XRD patterns were in line with those of origin state. Given the above information, we deduced the mechanochromism and thermochromism behavior were ascribed to crystalline-to-amorphous and crystalline-to-crystalline, respectively.

3.5. Discrimination of $CHCl_3$ assisted by UV irradiation

During the study of DDHAC in $CHCl_3$ solution, the photoinduced absorption and fluorescence changes were noticed. The double absorption peaks of DDHAC appeared at 442 nm and 464 nm in $CHCl_3$. In sharp contrast, after 120 s of exposure to UV lamp with 254 nm, the absorption band shifted to longer wavelength peaked at 484 nm and 515 nm with visible color change from yellow to pink (Fig. 4a). Meanwhile, distinct fluorescence change was also observed. The PL spectrum in $CHCl_3$ showed the emission maximum at 513 nm, with a further peak at 550 nm. Upon UV irradiation, a significantly weakened emission band peaked at 547 and 585 nm was monitored, leading to fluorescence change from green to faint pink (Fig. 4b). However, the photophysical properties of DDHAC in toluene, tetrahydrofuran, ethyl acetate, acetone, acetonitrile and methanol solutions were almost unchanged upon UV irradiation of 15 min. The comparison experiment indicated that the apparent changes of DDHAC in $CHCl_3$ solution under UV light could be triggered by $CHCl_3$ solvent. It was known that HCl can be generated upon exposure $CHCl_3$ to UV light [68], which would lead to protonation of the N atom from -NEt_2 group in the molecular structure [69]. Therefore, red shift of spectral bands of DDHAC in $CHCl_3$ after UV irradiation could be assigned to the interaction of this molecule with HCl. To prove the point, DDHAC in $CHCl_3$ solution toward HCl were conducted (Fig. 4). After 10 s of saturated HCl vapor fuming, the changing trends of the absorption and emission bands matched well with UV light irradiation results, further confirming the formation of DDHAC-H^+. These demonstrated DDHAC possessed promising $CHCl_3$-responsive property, and thereby it could be applied to discriminate $CHCl_3$ from organic solvents assisted by UV irradiation.

3.6. Protonation effect

Then the response of DDHAC in CH_3OH to HCl was tested (Fig. 5a). Upon 10 s of HCl fuming, distinct changes were found in Abs and PL spectra, corresponding to color change from orange to pink and fluorescence change from bright yellow to weak red. After being fumed with triethylamine (TEA), the color and fluorescence were recovered due to releasing of DDHAC molecule (Fig. S2 and Fig. 5a inset). Similar to solution state, DDHAC in solid state also exhibited sensitivity to HCl vapor (Fig. 5b). HCl fuming toward original samples resulted in strong fluorescence quenching, which could almost revert to original fluorescent intensity when the materials were treated with TEA. However, the TEA-fumed powders showed single emission peak. These results verify that DDHAC had a pronounced protonation effect.

4. Conclusions

In conclusion, we developed a multi-stimuli-responsive compound DDHAC based on Et_2N-substituted salicylaldehyde Schiff base with AIE and ESIPT characteristics. Owing to structural flexibility, the molecule showed mechanochromism and thermochromism. XRD results indicated that crystalline-to-amorphous and crystalline-to-crystalline conversions should be responsible for visible chromism response to mechanical and thermal stimuli, respectively. Additionally, protonation of the -NEt_2 group in DDHAC occurred upon HCl stimuli, resulting in acdichromism. This feature enabled DDHAC to differentiate of $CHCl_3$ from organic solvents assisted by UV irradiation, because $CHCl_3$ could generate HCl when exposed to UV light. We anticipated that the sample Et_2N-substituted salicylaldehyde Schiff base molecule would provide a new paradigm in design of multi-stimuli-responsive materials.

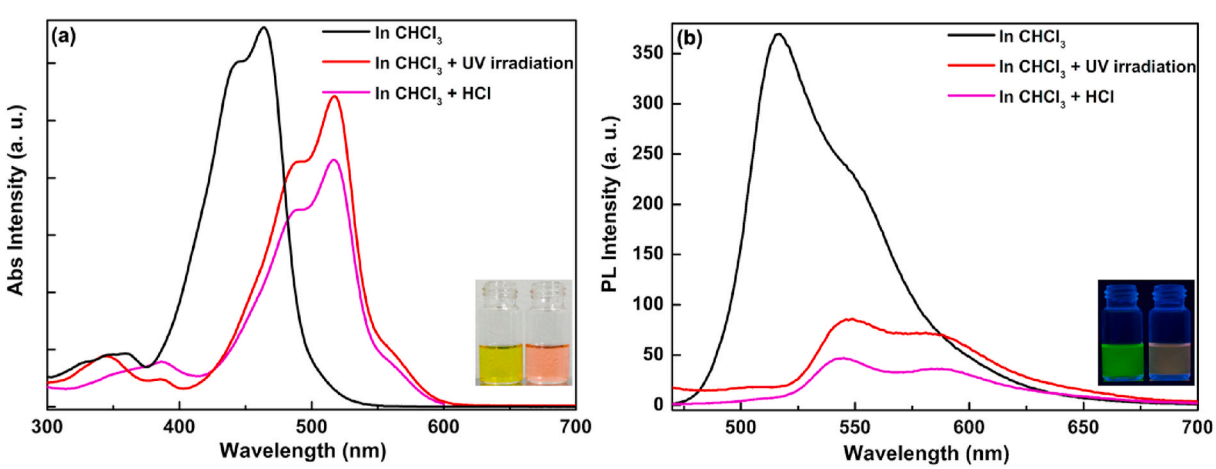

Fig. 4. (a) Absorption and (b) PL spectra of DDHAC in $CHCl_3$ with different stimuli. Inset: the photographs of DDHAC in $CHCl_3$ (left) and in $CHCl_3$ upon UV irradiation (right).

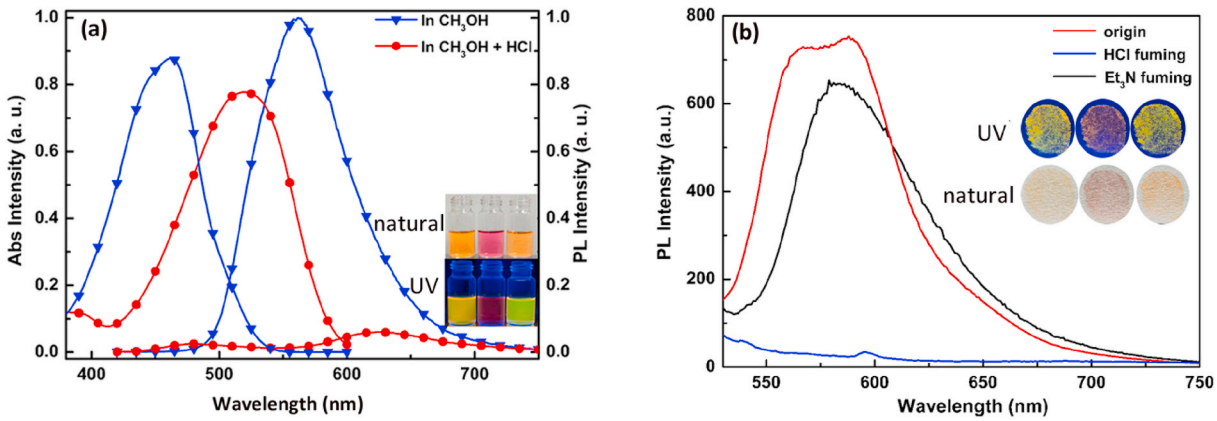

Fig. 5. (a) Absorption and PL spectra of DDHAC in CH_3OH before and after HCl fuming. Inset: the photographs of the initial (left), HCl fumed (middle) and TEA fumed (right) CH_3OH solution. (b) PL spectra of the initial, HCl fumed and TEA fumed powders. Inset: the photographs of DDHAC powder in original (left), HCl fumed (middle) and TEA fumed (right) state.

CRediT authorship contribution statement

Jun Shu: Investigation. **Tong Ni:** Investigation. **Xiaoqiang Liu:** Resources. **Bin Xu:** Resources. **Lang Liu:** Resources. **Wendao Chu:** Resources. **Kaiming Zhang:** Conceptualization, Writing – original draft. **Weidong Jiang:** Writing - review & editing, Supervision.

Declaration of competing interest

The authors declare that they have no known competing financial interests or personal relationships that could have appeared to influence the work reported in this paper.

Acknowledgements

This work was supported by the Sichuan University of Science and Engineering (Grant 2015RC25), Research Grant for Graduate Student of Chongqing University of Arts and Sciences (M2020ME27), Key Laboratory of Green Chemistry of Sichuan Institutes of Higher Education (Grant LZJ1807), and Chemical Synthesis and Pollution Control Key Laboratory of Sichuan Province (Grant CSPC 201908).

Appendix A. Supplementary data

Supplementary data to this article can be found online at https://doi.org/10.1016/j.dyepig.2021.109708.

References

[1] Liu H, Gu Y, Dai Y, Wang K, Zhang S, Chen G, Zou B, Yang B. Pressure-induced blue-shifted and enhanced emission: a cooperative effect between aggregation-induced emission and energy-transfer suppression. J Am Chem Soc 2020;142:1153–8.
[2] Chen Y, Zhang X, Wang M, Peng J, Zhou Y, Huang X, et al. Mechanofluorochromism, polymorphism and thermochromism of novel D–π–A piperidin-1-yl-substitued isoquinoline derivatives. J Mater Chem C 2019;7:12580–7.
[3] Liu X, Li A, Xu W, Ma Z, Jia X. An ESIPT-based fluorescent switch with AIEE, solvatochromism, mechanochromism and photochromism. Mater Chem Front 2019;3:620–5.
[4] Matsuo Y, Wang Y, Ueno H, Nakagawa T, Okada H. Mechanochromism, Twisted/folded structure determination, and derivatization of (N-phenylfluorenylidene) acridane. Angew Chem Int Ed 2019;58:8762–7.
[5] Wu X, Guo J, Cao Y, Zhao J, Jia W, Chen Y, et al. Mechanically triggered reversible stepwise tricolor switching and thermochromism of anthracene-o-carborane dyad. Chem Sci 2018;9:5270–7.
[6] Zhang K, Shu J, Chu W, Liu X, Xu B, Jiang W. Rational design of coumarin fluorophore with solvatochromism, AIE and mechanofluorochromic enhancement properties. Dyes Pigments 2021;185:108898.
[7] Xue P, Yang Z, Chen P. Hiding and revealing information using the mechanochromic system of a 2,5-dicarbazole-substituted terephthalate derivative. J Mater Chem C 2018;6:4994–5000.
[8] Yang X, Wang Q, Hu P, Xu C, Guo W, Wang Z, et al. Achieving remarkable and reversible mechanochromism from a bright ionic AIEgen with high specificity for mitochondrial imaging and secondary aggregation emission enhancement for long-term tracking of tumors. Mater Chem Front 2020;4:941–9.
[9] Yang Y, Li A, Ma Z, Liu J, Xu W, Ma Z, et al. Dibenzo[a,c]phenazine-phenothiazine dyad: AIEE, polymorphism, distinctive mechanochromism, high sensitivity to pressure. Dyes Pigments 2020;181:108575.
[10] Sagara Y, Takahashi K, Nakamura T, Tamaoki N. Mechanical and thermal stimuli-induced release of toluene included in luminescent crystals as one-dimensional solvent channels. J Mater Chem C 2020;8:10039–46.
[11] Huang L, Qian C, Ma Z. Stimuli-responsive purely organic room-temperature phosphorescence materials. Chem Eur J 2020;26:11914–30.
[12] Alam P, Leung NLC, Cheng Y, Zhang H, Liu J, Wu W, et al. Spontaneous and fast molecular motion at rom temperature in the solid state. Angew Chem Int Ed 2019;58:4536–40.
[13] Borbone F, Tuzi A, Panunzi B, Piotto S, Concilio S, Shikler R, et al. On–Off mechano-responsive switching of ESIPT luminescence in polymorphic N-salicylidene-4-amino-2-methylbenzotriazole. Cryst Growth Des 2017;17:5517–23.
[14] Zhang T, Han Y, Wang K, Liang M, Bian W, Zhang Y, et al. Alkyl chain-dependent ESIPT luminescent switches of phenothazine derivatives in response to force. Dyes Pigments 2020;172:107835.
[15] Shen S, Xia G, Jiang Z, Shao Q, Shan W, Wang H. Temperature controlling polymorphism and polymorphic interconversion in sublimation crystallization of 5-methoxy-salicylaldhyde azine. Cryst Growth Des 2019;19:320–7.
[16] Wei R, Song P, Tong A. Reversible Thermochromism of aggregation-induced emission-active benzophenone azine based on polymorph-dependent excited-state intramolecular proton transfer fluorescence. J Phys Chem C 2013;117:3467–74.
[17] Pei K, Zhou H, Yin Y, Zhang G, Pan W, Zhang Q, et al. Highly fluorescence emissive 5, 5'-distyryl-3, 3'-bithiophenes: synthesis, crystal structure, optoelectronic and thermal properties. Dyes Pigments 2020;179:108396.
[18] Yang W, Krantz KE, Freeman LA, Dickie DA, Molino A, Kaur A, et al. Stable borepinium and borafluorenium heterocycles: a reversible thermochromic "switch" based on boron-oxygen interactions. Chem Eur J 2019;25:12512–6.
[19] Liang S, Wang Y, Wu X, Chen M, Mu L, She G, et al. An ultrasensitive ratiometric fluorescent thermometer based on frustrated static excimers in the physiological temperature range. Chem Commun 2019;55:3509–12.
[20] Houjou H, Kato T, Huang H, Suzuki Y, Yoshikawa I, Mutai T. Re-evaluation of tert-butyl method in crystal engineering of salicylideneanilines by simultaneous observation of photochromism and thermochromism in single crystals. Cryst Growth Des 2019;19:1384–90.
[21] Okino K, Sakamaki D, Seki S. Dicyanomethyl radical-based near-infrared thermochromic dyes with high transparency in the visible region. ACS Mater Lett 2019;1:25–9.
[22] Yu B, Liu D, Wang Y, Zhang T, Zhang Y-M, Lia M, et al. A solid-state emissive and solvatofluorochromic fluorophore and its application in high-contrast, fast, and repeatable thermochromic blends. Dyes Pigments 2019;163:412–9.
[23] Zhang E, Hou X, Zhang Z, Zhang Y, Wang J, Yang H, et al. A novel biomass-based reusable AIE material: the AIE properties and potential applications in amine/ammonia vapors sensing and information storage. J Mater Chem C 2019;7:8404–11.
[24] Lee W, Lee D, Kim J-Y, Lee S, Yoon J. Imidazole and triazole head group-containing polydiacetylenes for colorimetric monitoring of pH and detecting HCl gas. Mater Chem Front 2018;2:291–5.
[25] Li XC, Wang CY, Wan Y, Lai WY, Zhao L, Yin MF, et al. A T-shaped triazatruxene probe for the naked-eye detection of HCl gas with high sensitivity and selectivity. Chem Commun 2016;52:2748–51.

[26] Nakane Y, Takeda T, Hoshino N, Sakai K-i, Akutagawa T. ESIPT fluorescent chromism and conformational Change of 3-(2-Benzothiazolyl)-4-hydroxy-benzenesulfonic acid by amine sorption. J Phys Chem C 2018;122:16249–55.
[27] Qiu Q-m, Gu L, Ma H, Yan L, Liu M, Li H. Double layer zinc–UDP coordination polymers: structure and properties. Dalton Trans 2018;47:14174–8.
[28] Sun XW, Wang ZH, Li YJ, Yang HL, Gong GF, Zhang YM, et al. Transparency and AIE tunable supramolecular polymer hydrogel acts as TEA-HCl vapor controlled smart optical material. Soft Matter 2020;16:5734–9.
[29] Xue P, Yao B, Shen Y, Gao H. Self-assembly of a fluorescent galunamide derivative and sensing of acid vapor and mechanical force stimuli. J Mater Chem C 2017;5:11496–503.
[30] Zhang Y, Yang H, Ma H, Bian G, Zang Q, Sun J, et al. Excitation wavelength dependent fluorescence of an ESIPT triazole derivative for amine sensing and anti-counterfeiting applications. Angew Chem Int Ed 2019;58:8773–8.
[31] Jarangdet T, Pratumyot K, Srikittiwanna K, Dungchai W, Mingvanish W, Techakriengkrai I, et al. A fluorometric paper-based sensor array for the discrimination of volatile organic compounds (VOCs) with novel salicylidene derivatives. Dyes Pigments 2018;159:378–83.
[32] Peng Z, Feng X, Tong B, Chen D, Shi J, Zhi J, et al. The selective detection of chloroform using an organic molecule with aggregation-induced emission properties in the solid state as a fluorescent sensor. Sensor Actuator B Chem 2016;232:264–8.
[33] Yang L, Xu X, Yu W, Li X, Zhang D. AIE-active shape-persistent macrocycles for the efficient discrimination of toluene. Dyes Pigments 2020;181:108612.
[34] Luo Y, Li C, Zhu W, Zheng X, Huang Y, Lu Z. A facile strategy for the construction of purely organic optical sensors capable of distinguishing D_2O from H_2O. Angew Chem Int Ed 2019;58:6280–4.
[35] Dong B, Lu Y, Song W, Kong X, Sun Y, Lin W. A dual-site controlled fluorescent sensor for the facile and fast detection of H_2O in D_2O by two turn-on emission signals. Chem Commun 2020;56:1191–4.
[36] Guragain S, Bastakoti BP, Malgras V, Nakashima K, Yamauchi Y. Multi-stimuli-responsive polymeric materials. Chemistry 2015;21:13164–74.
[37] Hu J, Dai L, Liu S. Analyte-reactive amphiphilic thermoresponsive diblock copolymer micelles-based multifunctional ratiometric fluorescent chemosensors. Macromolecules 2011;44:4699–710.
[38] Hua QX, Xin B, Liu JX, Zhao LX, Xiong ZJ, Chen T, et al. Bulky 4,6-disubstituted tetraphenylethene-naphthalimide dyad: synthesis, copolymerization, stimuli-responsive fluorescence and cellular imaging. Faraday Discuss 2017;196:439–54.
[39] Kelley EG, Albert JNL, Sullivan MO, Epps IIITH. Stimuli-responsive copolymer solution and surface assemblies for biomedical applications. Chem Soc Rev 2013;42:7057–71.
[40] Klajn R. Spiropyran-based dynamic materials. Chem Soc Rev 2014;43:148–84.
[41] Song Z, Wang K, Gao C, Wang S, Zhang W. A new thermo-, pH-, and CO_2-responsive homopolymer of poly[N-[2-(diethylamino)ethyl]acrylamide]: is the diethylamino group underestimated? Macromolecules 2015;49:162–71.
[42] Lavrenova A, Balkenende DW, Sagara Y, Schrettl S, Simon YC, Weder C. Mechano- and thermoresponsive photoluminescent supramolecular polymer. J Am Chem Soc 2017;139:4302–5.
[43] Zhuang J, Gordon MR, Ventura J, Li L, Thayumanavan S. Multi-stimuli responsive macromolecules and their assemblies. Chem Soc Rev 2013;42:7421–35.
[44] Zhang J, Li A, Zou H, Peng J, Guo J, Wu W, et al. A "simple" donor–acceptor AIEgen with multi-stimuli responsive behavior. Mater Horiz 2020;7:135–42.
[45] Wang M, Cheng C, Li C, Wu D, Song J, Wang J, et al. Smart, chiral, and nonconjugated cyclohexane-based bis-salicylaldehyde hydrazides: multi-stimuli-responsive, turn-on, ratiometric, and thermochromic fluorescence, single-crystal structures via DFT calculations. J Mater Chem C 2019;7:6767–78.
[46] Wang L, Xiong W, Tang H, Cao D. A multistimuli-responsive fluorescent switch in the solution and solid states based on spiro[fluorene-9,9'-xanthene]-spiropyran. J Mater Chem C 2019;7:9102–11.
[47] Roy B, Reddy MC, Hazra P. Developing the structure-property relationship to design solid state multi-stimuli responsive materials and their potential applications in different fields. Chem Sci 2018;9:3592–606.
[48] Fang W, Zhao W, Pei P, Liu R, Zhang Y, Kong L, et al. A Λ-shaped cyanostilbene derivative: multi-stimuli responsive fluorescence sensors, rewritable information storage and colour converter for w-LEDs. J Mater Chem C 2018;6:9269–76.
[49] Qian Y, Li S, Zhang G, Wang Q, Wang S, Xu H, et al. Aggregation-induced emission enhancement of 2-(2'-hydroxyphenyl)benzothiazole-based excited-state intramolecular proton-transfer compounds. J Phys Chem B 2007;111:5861–8.
[50] Tang W, Xiang Y, Tong A. Salicylaldehyde azines as fluorophores of aggregation-induced emission enhancement characteristics. J Org Chem 2009;74:2163–6.
[51] Feng Q, Li Y, Wang L, Li C, Wang J, Liu Y, et al. Multiple-color aggregation-induced emission (AIE) molecules as chemodosimeters for pH sensing. Chem Commun 2016;52:3123–6.
[52] Mutai T, Tomoda H, Ohkawa T, Yabe Y, Araki K. Switching of polymorph-dependent ESIPT luminescence of an imidazo[1,2-a]pyridine derivative. Angew Chem Int Ed 2008;47:9522–4.
[53] Pasha SS, Yadav HR, Choudhury AR, Laskar IR. Synthesis of an aggregation-induced emission (AIE) active salicylaldehyde based Schiff base: study of mechanoluminescence and sensitive Zn(ii) sensing. J Mater Chem C 2017;5:9651–8.
[54] Xie Y, Yan L, Tang Y, Tang M, Wang S, Bi L. A smart fluorescent probe based on salicylaldehyde schiff's base with AIE and ESIPT characteristics for the detections of N_2H_4 and ClO^-. J Fluoresc 2019;29:399–406.
[55] Knyazhansky MI, Metelitsa AV, AJa Bushkov, Aldoshin SM. Role of structural flexibility in fluorescence and photochromism of the salicylideneaniline: the "aldehyde" ring rotation. J Photochem Photobiol Chem 1996;97:121–6.
[56] Staehle IO, Rodríguez-Molina B, Khan SI, Garcia-Garibay MA. Engineered photochromism in crystalline salicylidene anilines by facilitating rotation to reach the colored trans-keto form. Cryst Growth Des 2014;14:3667–73.
[57] Zhang K, Shu J, Li J, Meng L, Yang Y, Xu B, et al. H-aggregate triggered mechanochromic luminescence property of 7-(diethylamino)-coumarin-3-carbaldehyde oxime derivative. Tetrahedron Lett 2020;61:151797.
[58] Sen Gupta A, Paul K, Luxami V. A fluorescent probe with "AIE + ESIPT" characteristics for Cu^{2+} and F^- ions estimation. Sensor Actuator B Chem 2017;246:653–61.
[59] Zhang T, Zhu L, Ma Y, Lin W. A near-infrared ratiometric fluorescent probe based on the C[double bond, length as m-dash]N double bond for monitoring SO_2 and its application in biological imaging. Analyst 2020;145:1910–4.
[60] Zhang X, Shi J, Shen G, Gou F, Cheng J, Zhou X, et al. Non-conjugated fluorescent molecular cages of salicylaldehyde-based tri-Schiff bases: AIE, enantiomers, mechanochromism, anion hosts/probes, and cell imaging properties. Mater Chem Front 2017;1:1041–50.
[61] Shellaiah M, Wu Y-H, Singh A, Raju MVR, Lin H-C. Novel pyrene- and anthracene-based Schiff base derivatives as Cu^{2+} and Fe^{3+} fluorescence turn-on sensors and for aggregation induced emissions. J Mater Chem 2013;1:1310–8.
[62] Peng L, Xu S, Zheng X, Cheng X, Zhang R, Liu J, et al. Rational design of a red-emissive fluorophore with AIE and ESIPT characteristics and its application in light-up sensing of esterase. Anal Chem 2017;89:3162–8.
[63] Zhang W, Ma Z, Li W, Li G, Chen L, Liu Z, et al. Discovery of quinazoline-based fluorescent probes to α1-adrenergic receptors. ACS Med Chem Lett 2015;6:502–6.
[64] Furukawa S, Shono H, Mutai T, Araki K. Colorless, transparent, dye-doped polymer films exhibiting tunable luminescence color: controlling the dual-color luminescence of 2-(2′-Hydroxyphenyl)imidazo[1,2-a]pyridine derivatives with the surrounding matrix. ACS Appl Mater Interfaces 2014;6:16065–70.
[65] Cao J, Liu Q-M, Bai S-J, Wang H-C, Ren X, Xu Y-X. Ladder-type dye with large transition dipole moment for solvatochromism and microphase visualization. ACS Appl Mater Interfaces 2019;11:29814–20.
[66] Mei J, Hong Y, Lam JWY, Qin A, Tang Y, Tang B. Aggregation-induced emission: the whole is more brilliant than the parts. Adv Mater 2014;26:5429–79.
[67] Ma Y, Yang Li, Chen L, Xiong Y, Yin G. Cyano-functionalized 1,4-bis((E)-2-(1H-indol-3-yl)vinyl)benzenes with aggregation induced emission characteristic and diverse thermochromic behavior. Dyes Pigments 2016;126:194–201.
[68] Peng Z, Feng X, Tong B, Chen D, Shi J, Zhi J, et al. The selective detection of chloroform using an organic molecule with aggregation-induced emission properties in the solid state as a fluorescent sensor. Sensor Actuator B Chem 2016;232:264–8.
[69] Jana S, Dalapati S, Guchhait N. Proton transfer assisted charge transfer phenomena in photochromic Schiff bases and effect of $-NEt_2$ groups to the anil Schiff bases. J Phys Chem 2012;116:10948–58.